Temperature and Ligand Dependence of Conformation and Helical Order in Myosin Filaments

S. Xu,[‡] G. Offer,[‡,§] J. Gu,[‡] H. D. White,[||] and L. C. Yu*[,‡]

Laboratory of Muscle Biology, National Institute of Arthritis, Musculoskeletal and Skin Diseases, National Institutes of Health, Bethesda, Maryland 20892, Department of Physiology, University of Bristol, University Walk, Bristol BS8 1TD, U.K., and Department of Physiological Sciences, Eastern Virginia Medical School, Norfolk, Virginia 23501

Received May 7, 2002; Revised Manuscript Received July 29, 2002

ABSTRACT: Mammalian myosin filaments are helically ordered only at higher temperatures (>20 °C) and become progressively more disordered as the temperature is decreased. It had previously been suggested that this was a consequence of the dependence of the hydrolytic step of myosin ATPase on temperature and the requirement that hydrolysis products (e.g., ADP·P_i) be bound at the active site. An alternative hypothesis is that temperature directly affects the conformation of the myosin heads and that they need to be in a particular conformation for helical order in the filament. To discriminate between these two hypotheses, we have studied the effect of temperature on the helical order of myosin heads in rabbit psoas muscle in the presence of nonhydrolyzable ligands. The muscle fibers were overstretched to nonoverlap such that myosin affinity for nucleotides was not influenced by the interaction of myosin with the thin filament. We show that with bound ADP·vanadate, which mimics the transition state between ATP and hydrolysis products, or with the ATP analogues AMP-PNP or ADP·BeF_x the myosin filaments are substantially ordered at higher temperatures but are reversibly disordered by cooling. These results reinforce recent studies in solution showing that temperature as well as ligand influence the equilibrium between multiple myosin conformations [Málnási-Csizmadia, A., Pearson, D. S., Kovács, M., Woolley, R. J., Geeves, M. A., and Bagshaw, C. R. (2001) *Biochemistry 40*, 12727−12737; Málnási-Csizmadia, A., Woolley, R. J., and Bagshaw, C. R. (2000) *Biochemistry 39*, 16135−16146; Urbanke, C., and Wray, J. (2001) *Biochem. J. 358*, 165−173] and indicate that helical order requires the myosin heads to be in the closed conformation. Our results suggest that most of the heads in the closed conformation are ordered, and that order is not produced in a separate step. Hence, helical order can be used as a signature of the closed conformation in relaxed muscle. Analysis of the dependence on temperature of helical order and myosin conformation shows that in the presence of these analogues one ordered (closed) conformation and two disordered conformations with distinct thermodynamic properties coexist. Low temperatures favor one disordered conformation, while high temperatures favor the ordered (closed) conformation together with a second disordered conformation.

Mammalian and avian myosin filaments show a remarkable dependence of structure on temperature (*4*−*11*). Above 20 °C, the X-ray diffraction pattern of relaxed rabbit skeletal muscle is similar to that of frog muscle, indicating that the myosin heads are helically arranged on the surface of the filament with an axial translation of 143 Å and a repeat of 429 Å (*4*, *11*). However, the X-ray pattern indicates increasing disorder as the muscle is cooled. In the ordered state, the heads lie on the filament surface and their motion is restricted, while in the disordered state, the heads are more mobile (*6*, *9*). The degree of order is also markedly dependent on the ligand bound to myosin (*4*, *11*, *12*). Disorder occurs at all temperatures in the absence of nucleotide or with bound ADP, GTP, or ATPγS,[1] while CTP promotes order more than ATP.

Wray (*4*) initially suggested that the temperature dependence of helical order might arise if it required ADP and P_i rather than ATP to be bound at the active site. The M·ATP $\rightleftarrows$ M·ADP·P_i equilibrium is temperature-dependent (*11*, *13*, *14*) so that at low temperatures M·ATP predominates and at high temperatures, M·ADP·P_i. In apparent support of this hypothesis, we found only small differences between K_{hyd}^{app}, the equilibrium constant for the hydrolytic step for rabbit myosin subfragment-1 in solution, and K_{ord}^{app}, the equilibrium constant for the disorder−order transition in relaxed rabbit psoas muscle (*11*).

An alternative hypothesis for explaining the effect of ligands and temperature on helical order is that myosin with a bound ligand undergoes conformational changes with

* To whom correspondence should be addressed. E-mail: yule@mail.nih.gov.

[‡] National Institutes of Health.

[§] University of Bristol.

[||] Eastern Virginia Medical School.

[1] Abbreviations: CTP, cytosine triphosphate; NTP, nucleoside triphosphate; NDP, nucleoside diphosphate; ATPγS, adenosine 5′-*O*-(γ-thiotriphosphate); AMP-PNP, 5′-adenylylimidodiphosphate; Ap5A, P^1,P^5-di(adenosine-5′)pentaphosphate; M, myosin; S1, myosin subfragment-1.

10.1021/bi026085t CCC: $25.00
Published on Web 12/19/2002

temperature and that helical order requires only one of those conformations. Although there is clear evidence from both studies in solution and X-ray crystallography that myosin heads adopt different conformations (*1*−*3*, *15*−*26*), the long-held view was that each nucleotide (ligand) absolutely determines the conformation of the myosin head. However, using tryptophan fluorescence as a monitor of conformation, it has recently been shown that myosin conformation is also markedly sensitive to temperature and that myosin with a given ligand bound exists in several conformations in equilibrium, the proportion of these depending on the temperature as well as on the ligand (*1*−*3*, *23*). Recent studies on a *Dictyostelium* S1 mutant with a single tryptophan in the relay loop (*1*, *2*) have strikingly confirmed earlier studies on rabbit myosin (*15*), suggesting that myosin heads can adopt three different conformations in solution. In the presence of ATP the following equilibria are present:

$$\mathrm{M} + \mathrm{ATP} \rightleftarrows \mathrm{M{\cdot}ATP} \rightleftarrows \mathrm{M^{\dagger}{\cdot}ATP} \rightleftarrows \mathrm{M^{*}{\cdot}ATP} \rightleftarrows \mathrm{M^{*}{\cdot}ADP{\cdot}P_i} \quad (1)$$

where M is the apo conformation, $M^{\dagger}$ is a conformation with slightly reduced fluorescence, and M* is a conformation with high fluorescence.[2] The second equilibrium is essentially irreversible, so the $M^{\dagger}$ and M* conformations dominate. The hydrolysis of ATP at the active site and the conformational change from $M^{\dagger}$ to M*, previously supposed to be coincident, are separate processes which are not absolutely coupled. So after ATP hydrolysis, the heads are largely in the M* conformation, but before hydrolysis, both $M^{\dagger}$ and M* conformations coexist, the proportions depending on temperature.

These solution conformations can be compared with the three conformations (open, closed, and "detached") of the myosin head determined by X-ray crystallography (*18*, *19*, *21*, *25*−*27*). These differ in the position of the four subdomains comprising the motor domain of the head. In the absence of nucleotides, the head crystallizes in the open conformation, regardless of species (*24*, *26*, *27*). Hence, the M (apo) solution conformation can be assigned to the open crystal conformation (*26*). With analogues, like ADP·V_i and ADP·AlF_4, of the transition state between ATP and its products, the head crystallizes in the closed conformation regardless of species (*18*, *19*, *21*, *26*). So the M* solution conformation can be assigned to the closed crystal conformation. The $M^{\dagger}$ solution conformation may tentatively be assigned to the third, detached crystal conformation (*25*, *26*). However, this assignment is more controversial, and we shall therefore discuss our results primarily in terms of the solution conformations rather than the crystal conformations. In particular, we will refer to the equilibrium constant for the $M^{\dagger} \rightleftarrows M^{*}$ transition as $K_{\dagger *}^{\mathrm{app}}$.

We have previously pointed out that helical order and the proportion of heads in the M* (closed) conformation have a similar dependence on temperature and on the nature of the ligand (*11*), suggesting that helical order requires the myosin heads to be in the M* (closed) conformation. This hypothesis needs to be tested. In this paper, we investigate further by X-ray fiber diffraction how temperature affects helical order in rabbit skeletal muscle. In our previous experiments (*11*), variation of order with temperature was accompanied by changes in bound ligand (for example ATP to ADP·P_i) due to hydrolysis, and the effect of temperature was not tested independently of ligand. Our aim in this study was to discriminate between the alternative hypotheses (1) that temperature affects helical order by changing myosin conformation or (2) that it does so by altering the proportion of myosin heads with hydrolysis products bound at the active site. First, we have used ligands that are not hydrolyzed. We found that when the myosin heads are complexed with ADP·V_i to mimic the transition state between ATP and ADP·P_i (*4*, *19*, *28*, *29*), or with the ATP analogues AMP-PNP and ADP·BeF_x (*18*, *30*, *31*), the heads are well ordered at high temperatures but become disordered on cooling. In addition, we reanalyzed our data (*11*) on the variation with temperature of $K_{\mathrm{ord}}^{\mathrm{app}}$ and $K_{\mathrm{hyd}}^{\mathrm{app}}$. On the basis of eq 1, the variation with temperature of $K_{\mathrm{hyd}}^{\mathrm{app}}$ and $K_{\dagger *}^{\mathrm{app}}$ is compared with $K_{\mathrm{ord}}^{\mathrm{app}}$. Our results support the hypothesis that temperature affects helical order by changing the myosin conformation. Our work also supports the view that myosin with a ligand bound exists in several conformations, the proportions of which depend on temperature as well as ligand, rather than the view that each ligand produces a single myosin conformation.

MATERIALS AND METHODS

Muscle Preparation and Solutions. (1) Muscle Fibers Stretched to Nonoverlap. All experiments were performed on chemically skinned bundles of rabbit M psoas major stretched to nonoverlap. It was shown that the nucleotide affinity for myosin attached to actin was affected by the state of activation of the thin filament ("turned on" or "turned off") (*32*, *33*). To minimize possible complications due to actin−myosin interactions or thin filament activation, all experiments were performed at a nonoverlap sarcomere length (4.2 μm). For the nonoverlap experiments, the bundle with an initial sarcomere length of 2.4 μm was stretched to a sarcomere length of 4.2 μm in the skinning solution at 5 °C over the course of 3−4 h by a motor (Micro Mo Electronics Inc., St. Petersburg, FL; controller by Acrotech, Pittsburgh, PA. Some X-ray diffraction patterns were taken of bundles with a sarcomere length of 2.4 μm under relaxed and rigor conditions. The sarcomere length was monitored by laser light diffraction during stretch. Only those stretched bundles giving a sharp laser pattern and without a single broken fiber were used. The integrity of the fibers was always checked under the microscope immediately before the experiments (*11*).

(2) Solutions. The following solutions were used. (1) Relaxing (MgATP) solution contained 2 mM MgATP, 2 mM $MgCl_2$, 2 mM EGTA, 5 mM DTT, 10 mM imidazole, 10 mM creatine phosphate, and 133 mM potassium propionate [pH 7.0, ionic strength (μ) = 170 mM]. To complete the ATP-backup system, 109 units of creatine phosphokinase (CPK)/mL was present.

(2) Rigor solution contained 2.5 mM EGTA, 2.5 mM EDTA, 10 mM imidazole, 5 mM DTT, and 150 mM potassium propionate (pH 7.0, μ = 170 mM).

[2] To avoid confusion, we shall use the same terminology for the three solution conformations of vertebrate myosin that were used for *Dictyostelium* myosin, rather than using the older terminology, M, M*, and M** (*15*).

(3) NTP-free solution contained 2 mM EGTA, 4 mM $MgCl_2$, 10 mM imidazole, 50 mM glucose, 147 mM potassium propionate, 5 mM DTT, 2 units/mL hexokinase, and 0.25 mM Ap5A (pH 7.0, $\mu = 170$ mM).

(4) AMP-PNP-containing solution was made by adding 2 mM AMP-PNP to the NTP-free solution with the final ionic strength adjusted to 170 mM. This was achieved similarly for the ADP·V_i-containing solution by adding 2 mM ADP and 3 mM Na_3VO_4 and for the ADP·BeF_x-containing solution by adding 2 mM ADP, 2 mM $BeCl_2$, and 10 mM NaF. A stock orthovanadate solution was prepared according to the method described in ref *34*. $BeCl_2$ and NaF solutions were prepared according to the methods described in ref *35*.

Before the rigor solution or NTP-free solution was applied, the bundles were rinsed several times with a "quick rinse" solution containing 5 mM EGTA, 15 mM EDTA, and 20 mM imidazole (pH 7.0, $\mu = 70$ mM) (*36*, *37*). The fiber bundles were immersed in solutions containing nonhydrolyzable ligand for 20−30 min before the X-ray patterns were taken. The temperature of the bathing solution in the chamber was maintained at the preset temperatures ± 1 °C by two thermal electric devices controlled by a feedback circuit by Cambion (Cambridge, MA). The temperature ranged between 5 and 35 °C.

X-ray Source, Camera, and Detector System. The experiments were performed at beamline X27C (Advanced Polymer PRT) at the National Synchrotron Light Source (NSLS), Brookhaven National Laboratory (BNL), Upton, NY. The specimen-to-detector distance was 1500 mm. A MAR Research CCD detector or imaging plate detector (Hamburg, Germany) with a pixel size of 0.1 mm × 0.1 mm was used for collecting the X-ray data (for details, see ref *38*). The spacings of all reflections were calibrated by the 1/144.3 $Å^{-1}$ meridional reflection from skinned rabbit psoas muscle in rigor at $\mu = 170$ mM and 25 °C (see ref *10* for details).

Data Reduction and Analysis. The data in the four quadrants were first rotated, folded, and averaged. The program analyzed slices parallel either to the meridian or to the equator of the diffraction patterns, summing the intensities across the slices to generate one-dimensional intensity profiles for further analysis. For following the distribution of intensity along layer lines, the widths of the slices were chosen so the entire widths of the layer lines would be included.

To compare directly the intensities obtained under different conditions with minimum error, diffraction patterns were always recorded from the same bundle for all the conditions of interest (e.g., the temperature change from 5 to 35 °C). To compare quantitatively the data from different bundles with different sizes and to input all data for statistical analysis, the integrated intensity of the first myosin layer line obtained under the condition of relaxing solution at 25 °C was used for normalization. To correct for contributions from the thin filament and the thick filament backbone to myosin layer lines, difference patterns were obtained; the patterns obtained in the absence of nucleotide were subtracted from those in the presence of ligands. Integrated intensities of the first myosin layer line in the difference patterns were obtained with the program PCA (Oxford Instrument, Oak Ridge, TN).

Estimated Mass Distributed in the Helical Array. The layer lines in the difference patterns index on the 430 Å repeat and therefore arise from the myosin filament alone. Consequently, the intensities of the myosin layer lines are directly proportional to the square of the mass of the myosin heads in the helical array scattering coherently. The equilibrium constant of the disorder ⇄ order transition is defined as

$$K_{\mathrm{ord}}^{\mathrm{app}} = \frac{a}{1-a}$$

where a is the fraction of the heads in the ordered state. In our earlier study on the disorder ⇄ order transition of the myosin filament, the fraction of heads in the ordered state in ATP at 25 °C was determined to be 0.93 (*11*). Hence, to derive the fraction in the ordered state in a ligand at any temperature T, the amplitude obtained under these conditions was divided by the amplitude obtained in the presence of ATP at 25 °C and multiplied by 0.93.

The dependence on temperature of the equilibrium constants for the disorder ⇄ order transformation or a conformational change can be expressed by the van't Hoff equation:

$$\ln K = \frac{-\Delta H^\circ}{RT} + \frac{\Delta S^\circ}{R}$$

where K is the equilibrium constant, T is the absolute temperature, R is the gas constant, ΔH° is the enthalpy of the transition, and ΔS° is the entropy change. The dependencies on temperature of these equilibrium constants were fit using the nonlinear least-squares fitting routines in the software package Scientist (Micromath, Ogden, Utah).

RESULTS

Effect of Temperature on Helical Order in the Presence of ATP Analogues. ADP·BeF_x and AMP-PNP were used as the ATP analogues (*18*, *31*). According to the hypothesis that helical order requires hydrolysis products to be bound at the active site, there should be no helical order of the myosin heads in the presence of these analogues. At 15 °C, the intensity of the myosin layer lines with both these ATP analogues was low (Figure 1A), and if the mixture were cooled to 5 °C, the myosin layer lines became very weak, showing little helical order (intensity too weak to be measured accurately). However, at 25 °C with either of these ATP analogues, we observed clear myosin layer lines indexing on an ∼430 Å repeat extending out to the sixth layer line (Figure 1B). These are similar to those obtained in the presence of ATP at these temperatures, although they are not as strong (intensity ∼25% of that in ATP at 25 °C). Once the mixture had warmed to a higher temperature (∼35 °C), there was only a little change in intensity with either of these analogues (Figure 1C). The intensity profiles parallel to the meridian showed that the intensity of all myosin layer lines diminished by a similar factor on cooling. Although the intensity of the first myosin layer line is lower in the presence of the ATP analogues than in ATP (Figure 2A), the profiles along this layer line are very similar (Figure 2B), indicating that the same helical structure is present. We calculated $K_{\mathrm{ord}}^{\mathrm{app}}$, in the ATP analogues at each temperature, by comparing the amplitude of the layer lines with that obtained in ATP at 25 °C. van't Hoff plots of $\ln K_{\mathrm{ord}}^{\mathrm{app}}$ versus $1/T$ for the ATP analogues and ATP are compared in Figure 3A. The plots for the ATP analogues are markedly curved,

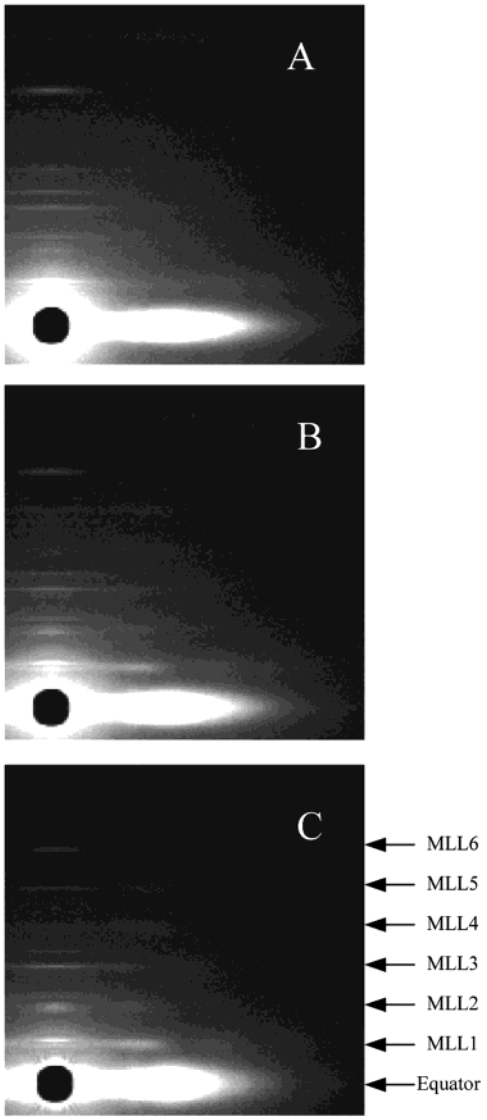

FIGURE 1: Comparison of the low-angle X-ray diffraction patterns of a single bundle of permeabilized rabbit psoas muscle fibers in ADP·BeF$_x$. The temperature was increased in the following order: (A) 15, (B) 25, and (C) 35 °C. The sarcomere length was 4.1 μm. The myosin layer lines are marked by MLL1−6.

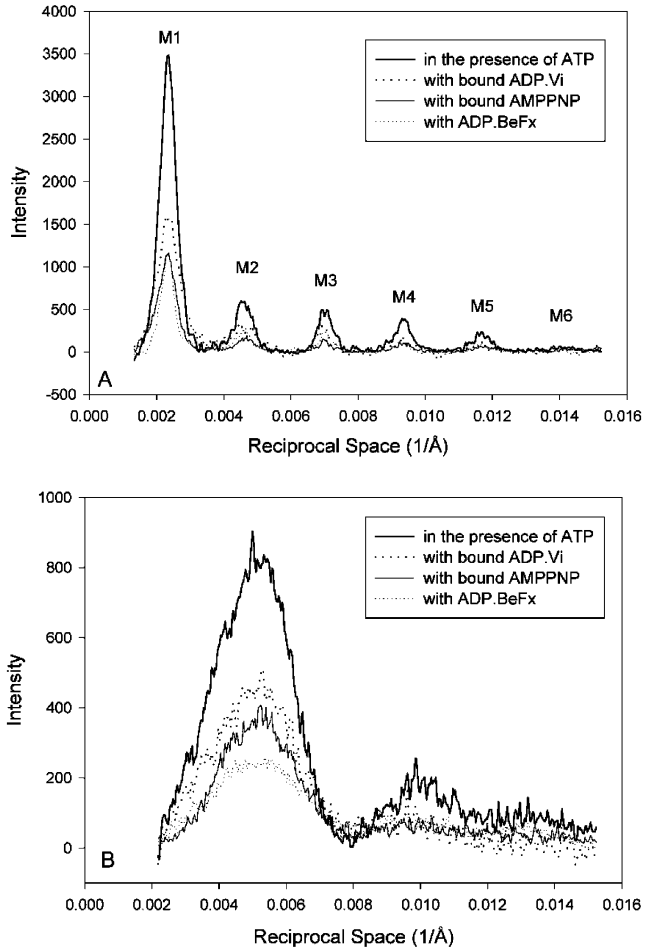

FIGURE 2: Comparison of the intensities of the myosin layer lines in the presence of different ligands at 25 °C. (A) Profiles of the integrated intensity in a slice parallel to the meridian from 0.00280 to 0.00795 Å^{-1} (R). (B) Profiles of the integrated intensity along the first myosin layer line in the presence of ATP (thick line), with bound ADP·V$_i$ (dashed line), with bound AMP-PNP (thin line), and with bound ADP·BeF$_x$ (dotted line). The profiles in the top two lines were obtained from the same bundle and those in the bottom two from different bundles. All of the intensities were first normalized by the intensities of the first myosin layer lines of the individual bundles in the presence of ATP at 25 °C, obtained at the beginning of the experiments (see Materials and Methods).

and although at low temperatures they have the same slope as with ATP, at >20 °C they plateau. This could not be due to the ligand affinity changing with temperature, since the concentrations used in the experiments were several orders of magnitude in excess of the affinity of myosin for the ligands (*39*, *40*), and modulation of the affinity by thin filaments (*32*, *33*) could not occur in the overstretched fibers. At all temperatures, the plots for the ATP analogues fall below the plot for ATP, consistent with the observations (*12*) that higher temperatures are required for the appearance of ordered heads with bound ADP·BeF$_x$.

Our observation that substantial helical order is present with nonhydrolyzable ATP analogues at high temperatures strongly favors the hypothesis that the ordered state requires the heads to be in the closed conformation, rather than the hypothesis that the ordered state requires the products ADP·P$_i$ to be bound in the active site (see the Discussion).

Effect of Temperature on Helical Order in the Presence of a Transition State Analogue. ADP·V$_i$ is an analogue of the transition state rather than the products. However, it appears likely that the conformation of myosin with bound products is the same as with bound ADP·V$_i$ (*22*). Therefore, according to the hypothesis that helical order requires products bound at the active site, in the presence of the ADP·V$_i$ the heads should be fully ordered at all temperatures. With bound ADP·V$_i$ at higher temperatures (∼25 °C), we did indeed observe strong myosin layer lines indexing on an ∼430 Å repeat extending out to the sixth layer line. These were stronger (intensity ∼50% of that in ATP at 25 °C) than those obtained with AMP-PNP and ADP·BeF$_x$. This is similar to the result in ref *41* which showed that in *frog* muscle the patterns with ATP and ADP·V$_i$ were similar. On warming to 30 °C, there was no increase in the intensity of the myosin layer lines and possibly even a slight decrease at 35 °C. On cooling to 20 °C, there was little change in intensity. This insensitivity of the intensity over the temperature range of 20−35 °C is similar to previous observations (*4*). However, with further cooling to 5 °C, the layer lines became very weak, showing that very little order

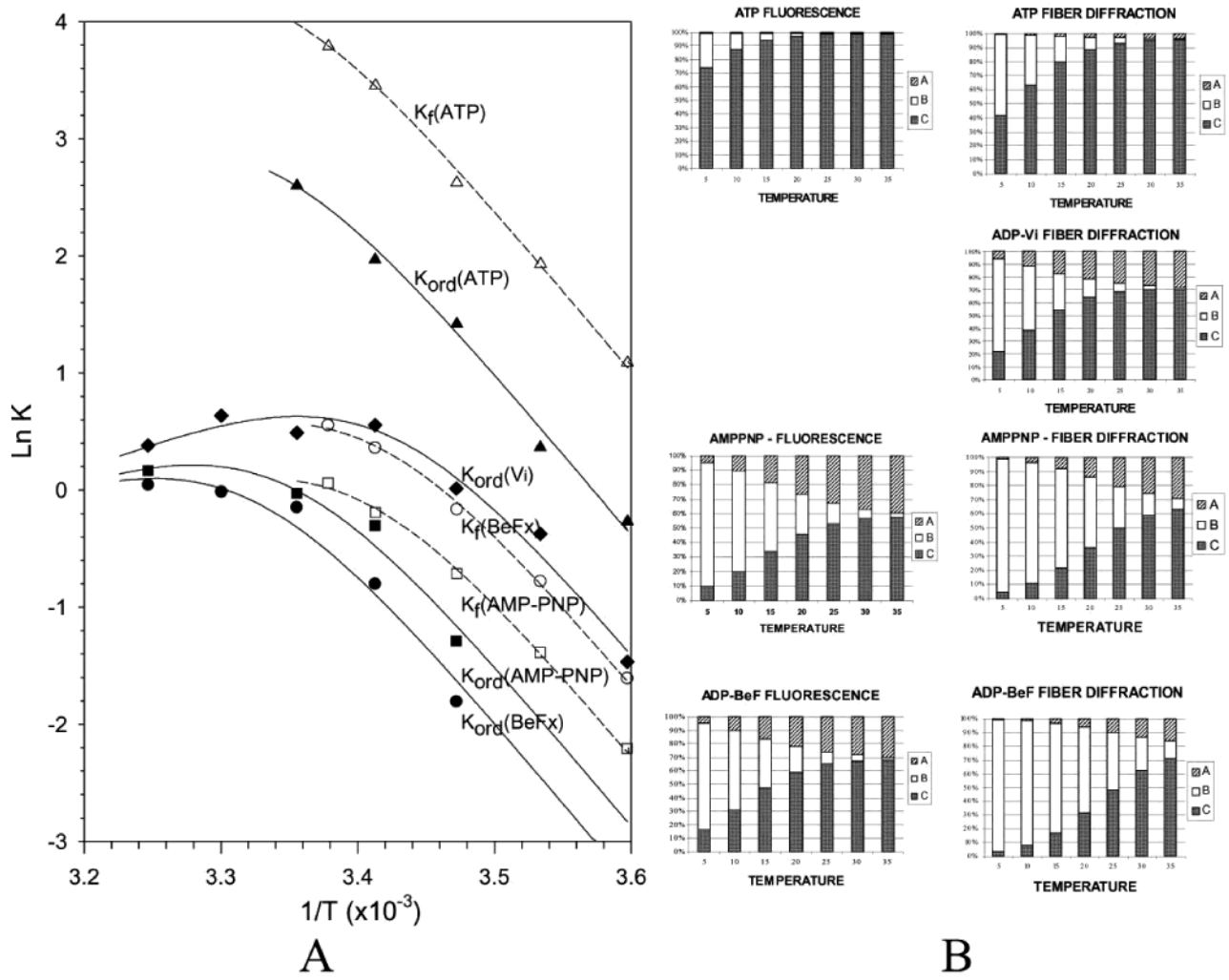

FIGURE 3: Effect of temperature on the disorder ⇄ order transition in rabbit myosin filaments and on the conformational change in the W501+ mutant of *Dictyostelium* S1 measured by fluorescence (data from ref *1*). (A) van't Hoff plots. The X-ray diffraction experimental points K_{ord} for the disorder ⇄ order transition are (i) in the presence of ATP, (ii) with bound ADP·V_i, (iii) with bound AMP-PNP, and (iv) with bound ADP·BeF_x. The fluorescence data for the conformational change K_f are (v) in the presence of ATP, (vi) with bound AMP-PNP, and (vii) with bound ADP·BeF_x. The lines are theoretical lines: $\Delta H_{AB} = -154$ kJ/mol and $\Delta H_{BC} = 116$ kJ/mol with ΔS_{AB} and ΔS_{BC} values in Table 1 chosen to best fit the data. (B) Bar graphs showing the proportion of the three states (A−C) as a function of the temperature which best fit the data for the ligands ATP, AMP-PNP, ADP·BeF_x, and ADP·V_i for both fluorescence (left column) and X-ray fiber diffraction (right column).

remained. The effect of cooling was reversible; when the fiber bundle was rewarmed to higher temperatures, the intensity of the layer lines was restored even after unbound ADP·V_i had been washed out (Figure 4). This not only shows that the change is reversible but also shows that the ADP·V_i binds very tightly to and dissociates very slowly from the active site of myosin in fibers, stretched beyond overlap, as had previously been observed in solution (*34*). At 20 °C, the half-time for the formation of complexes of myosin with ADP·V_i, ADP·BeF_x, and ADP·F_x and AMP-PNP is <1 min, but dissociation occurs over several days.

The intensity distribution along the first myosin layer line is shown in Figure 2B and compared with that in ATP. Although the intensity is lower in the presence of ADP·V_i than in the presence of ATP, the profiles are similar and the radial position of the main peak remains the same, indicating that the same helical structure is present. In Figure 3A, a van't Hoff plot of K_{ord}^{app} for ADP·V_i is compared with our previous data in the presence of ATP (*11*). The plot for ADP·V_i is markedly curved with the helical order reaching a maximum at 20−30 °C with some suggestion of a decline at higher temperatures. At all temperatures, the plot for ADP·V_i falls below that for ATP but above that for the ATP analogues.

Our observation that helical order varies with temperature even with ADP·V_i bound again strongly favors the hypothesis that the ordered state requires the heads to be in the M* (closed) conformation rather than the hypothesis that the ordered state requires the products ADP·P_i to be bound in the active site.

Analysis of van't Hoff Plots. Figure 3A compares the dependence on temperature of K_{ord}^{app} with that of $K_{\dagger*}^{app}$, with bound ADP·BeF_x, with bound AMP-PNP, and in the presence of ATP. The plots are nonlinear at higher temperatures for all the data. As stated in Effect of Temperature on Helical Order in the Presence of ATP Analogues, the nonlinearity could not be due to weaker ligand affinity at the higher temperatures. The simplest model that can accommodate this nonlinearity is one in which there are two disordered states, A and B, assumed to be of equally low

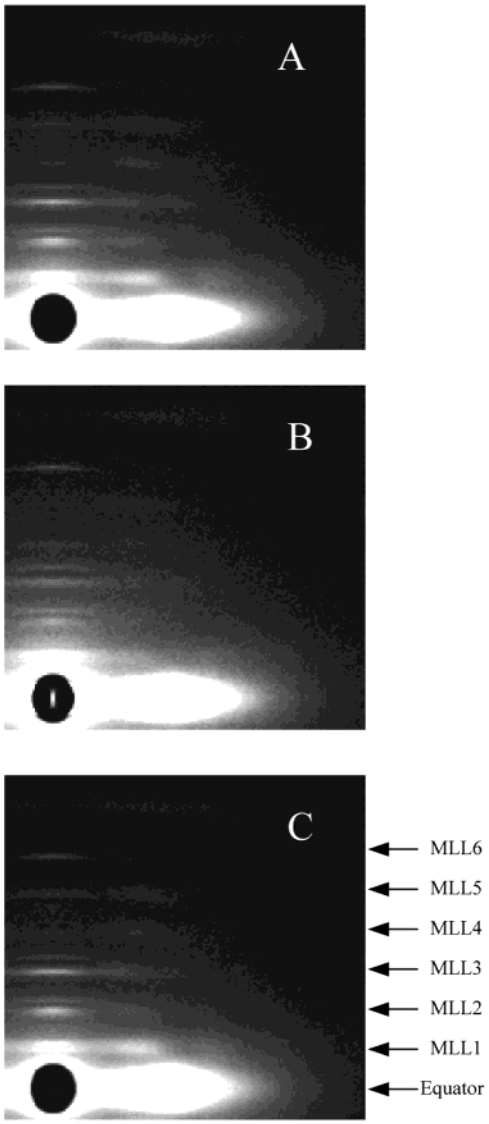

FIGURE 4: Reversibility of the effect of temperature on the X-ray diffraction pattern with bound ADP·V_i (A) at 20 °C showing strong myosin layer lines, (B) after cooling to 5 °C showing very weak myosin layer lines, and (C) after subsequent rewarming to 20 °C followed by washing out the unbound ADP·V_i with quick rinse solution and then a nucleotide-free solution. The sarcomere length was 4.1 μm.

fluorescence, in equilibrium with an ordered, high-fluorescence state C. Because the conformational data were obtained by observing the fluorescence of a single tryptophan residue in the relay loop, the implication is that C is the M* (closed) conformation and that the A and B states have conformations different from C.

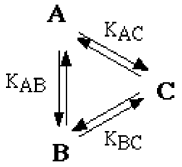

We distinguish between A and B by defining A as having the higher enthalpy so that ΔH_{AB} is negative. We depict these equilibria as a cyclic scheme because these data provide information about the thermodynamic properties of the intermediates in equilibrium but provide no information about the mechanism or sequence of the reaction.

Remarkably, good fits were obtained to the data with identical enthalpy changes (ΔH_{AB} and ΔH_{BC}) for all ligands and for both the conformational transition and the disorder $\rightleftarrows$ order transition. For all ligands, $\Delta H_{AB} \sim -154$ kJ/mol and $\Delta H_{BC} \sim 116$ kJ/mol (implying $\Delta H_{AC} \sim -38$ kJ/mol). The large enthalpy difference between the A and B states suggests that they have significantly different conformations. The differences in free energy (and thus equilibrium constant) characteristic of each of the ligands and myosins were assigned to differences in the entropy values (ΔS_{AB} and ΔS_{BC}). This produces a more robust fit than if all four parameters were allowed to vary independently for each curve. In practice, ΔH_{BC} determines the slope of the van't Hoff plots at low temperatures and ΔH_{AC} would determine the slope at high temperatures. The entropy values produce vertical displacements of the curves. The fit values are shown in Table 1. The fit values of K_{AB} are relatively insensitive to ligand, but those of K_{BC} and K_{AC} are much larger for ATP than for the analogues. This is consistent with the products ADP·P_i stabilizing the M* (closed) conformation more than ATP does. K_{BC} for ATP may not be significantly different if corrected by the value for the intrinsic equilibrium constant for the ATP hydrolysis step (81) determined in Reanalyzing Data on the Variation with Temperature of K_{ord}^{app} and K_{hyd}^{app} (see Table 1). The effect of temperature and ligand upon the distribution of the three states (A−C) for each ligand is shown in Figure 3B. At a low temperature (~5 °C) with AMP-PNP, ADP·BeF_x, or ADP·V_i, the predominant state is the low-enthalpy state B. As the temperature is increased, the proportion of the higher-enthalpy states A and C increases at the expense of B, so the helical order and fluorescence intensity increase. But as ΔH_{AC} is small, the [A]/[C] ratio is relatively insensitive to temperature, so even at high temperatures, C coexists with A, explaining why the van't Hoff plots of K_{ord}^{app} and $K_{\dagger*}^{app}$ plateau. In the presence of ATP, the fraction in the A state is small even at high temperatures. In summary, analyses of the van't Hoff plots indicate that for each bound nucleotide, myosin exists in three conformations.

Reanalyzing Data on the Variation with Temperature of K_{ord}^{app} and K_{hyd}^{app}. Another approach to discriminating between the two hypotheses is to compare over a range of temperatures the values of K_{ord}^{app} with K_{hyd}^{app} or $K_{\dagger*}^{app}$. If Wray's original 1987 hypothesis (that the ordered state requires the heads to have bound ADP·P_i) were correct, K_{ord}^{app} would equal K_{hyd}^{app}, whereas in the alternative hypothesis (that the ordered state requires the heads to be in the closed conformation), it would equal $K_{\dagger*}^{app}$. The Appendix gives a derivation of the variation with temperature of K_{hyd}^{app} and $K_{\dagger*}^{app}$ for the model of Málnási-Csizmadia et al. (*1*, *2*) (eq 1). Four parameters are required to define the equilibria: ΔH, the enthalpy change for the $M^{\dagger} \rightleftarrows M^*$ transition, K_{hyd}^*, the intrinsic equilibrium constant for ATP hydrolysis on the M* (closed) conformation, $K_{\dagger*}^{298}$, the intrinsic equilibrium constant at 298 K for the $M^{\dagger} \rightleftarrows M^*$ transition with bound ATP, and c, the coupling constant.

In Figure 5 are shown our previous experimental data (*11*) of the dependence on temperature of K_{hyd}^{app} and K_{ord}^{app} in the presence of ATP. The experimental points for K_{hyd}^{app} only

Table 1: Thermodynamic Parameters for the Isomerization of Conformations A−C with Different Ligands[a]

	ΔS_{AB} (kJ mol^{-1} K^{-1})	ΔG_{AB} (kJ/mol)	K_{AB} at 25 °C	ΔS_{BC} (kJ mol^{-1} K^{-1})	ΔG_{BC} (kJ/mol)	K_{BC} at 25 °C	K_{AC} at 25 °C	K_{AC} at 25 °C corrected for hydrolysis equilibrium
conformational transitions[b]								
AMP-PNP	−0.5225	1.7	0.5	0.3999	−2.9	3.2	1.6	
ADP·BeF$_x$	−0.5240	2.1	0.4	0.4050	−4.4	5.9	2.5	
ATP	−0.5123	−1.4	1.8	0.4271	−11.0	84.1	147.5	1.8
disorder ⇄ order transitions								
AMP-PNP	−0.5146	−0.7	1.3	0.3949	−1.4	1.7	2.3	
ADP·BeF$_x$	−0.5104	−2.0	2.2	0.3907	−0.1	1.1	2.3	
ADP·V$_i$	−0.5264	2.8	0.3	0.4072	−5.1	7.7	2.5	
ATP	−0.5122	−1.4	1.8	0.4155	−7.5	20.9	37.1	0.5

[a] Both sets of data were fitted with the following values: $\Delta H_{AB} = -154.1$ kJ/mol and $\Delta H_{BC} = 116.3$ kJ/mol. [b] The fluorescence data on a *Dictyostelium* mutant myosin head (*2*) were used to determine the thermodynamic parameters for the $M^{\dagger} \rightleftarrows M^*$ conformational transition.

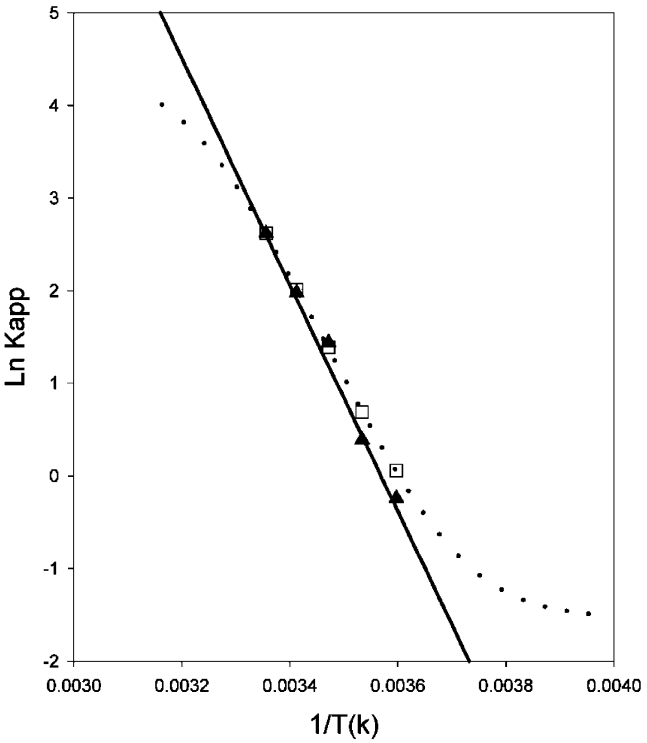

FIGURE 5: van't Hoff plots showing the effect of temperature in the presence of ATP on K_{ord}^{app}, the equilibrium constant for the disorder ⇄ order transition in rabbit myosin filaments, on $K_{\dagger *}^{app}$, the equilibrium constant for the $M^{\dagger} \rightleftarrows M^*$ transition, and on K_{hyd}^{app}, the equilibrium constant for the hydrolysis step in rabbit S1. The filled triangles are our experimental values for K_{ord}^{app} and the empty squares those for K_{hyd}^{app} (*11*). The theoretical line based on the loose coupling model that best fits the experimental values of K_{hyd}^{app} is represented by a dotted line and the theoretical line for $K_{\dagger *}^{app}$ in S1 (calculated with the same parameters) by a solid line (see the Appendix).

were fitted by adjusting the above four parameters to minimize the root-mean-square deviation in ln K_{hyd}^{app} between the experimental and theoretical values. The best fit (dotted line with an rms deviation of 0.012) was obtained with the following values: $\Delta H = 102$ kJ/mol, $K_{hyd}^{*} = 81$, $K_{\dagger *}^{298} = 0.20$, and $c = 376$. Although the fit is good, the data cannot be obtained over a sufficiently wide temperature range for a really stringent test to be made of this model. The value of $K_{\dagger *}^{298}$ of 0.20 implies that at 25 °C the $M^{\dagger} \rightleftarrows M^*$ transition with ATP bound is poised and slightly unfavorable. However, the coupling constant c is 376, so the equilibrium constant, $cK_{\dagger *}^{298}$, for the $M^{\dagger} \rightleftarrows M^*$ transition with products bound is 76, and the M* (closed) conformation is strongly favored. Although not infinite, the coupling constant c is $\gg 1$, so the $M^{\dagger} \rightleftarrows M^*$ transition and the hydrolysis steps are quite tightly coupled (*1*−*3*). The coupling constant of 376 implies that ADP·P$_i$ stabilizes the M* (closed) conformation more than ATP does by ∼15 kJ/mol. The same values for the four parameters were used to calculate the expected dependence on temperature for $K_{\dagger *}^{app}$ (solid line in Figure 5).

We previously noted that our data points for K_{ord}^{app} lie close to K_{hyd}^{app} and on this basis inferred that helical order required products to be bound at the active site (*11*). However, at lower temperatures there are differences, with K_{hyd}^{app} being ∼35% higher than K_{ord}^{app}. Our data points for K_{ord}^{app} lie closer to the theoretical line for $K_{\dagger *}^{app}$. While the errors in determining K_{ord}^{app} and K_{hyd}^{app} may not allow a decisive discrimination between the two hypotheses to be made on the basis of these data alone, the data can no longer be taken to favor the hypothesis that helical order requires that products be bound at the active site. Taken together with our experiments with the analogues, they provide additional support for the alternative hypothesis that the ordered state requires the heads to be in the closed conformation.

DISCUSSION

In this paper, we have studied by X-ray fiber diffraction the helical order of the myosin heads in the presence of several ligands that cannot be hydrolyzed. We were therefore able to isolate the effect of temperature on helical order from the effects of temperature on the hydrolysis equilibrium. Our studies on intact muscle have the advantage of using a physiological system. Many techniques (e.g., low-angle X-ray scattering) are stretched to their limits to detect conformational changes in myosin, but the changes in myosin layer line intensity from disorder to order as the temperature is increased are large and easily measured. Moreover, such measurements follow large-scale conformational changes in the myosin heads in native thick filaments and give insights into a regulatory mechanism that may control the interaction of myosin with actin in the myofilament lattice.

The M (Closed) Conformation Is Required for Helical Order.* When ADP·V$_i$ is bound at the active site of myosin in muscle at ∼25 °C, we observed that the myosin filaments were substantially ordered. This was not unexpected since the complex with bound ADP·V$_i$ is considered to be an analogue of the transition state between ATP and its hydrolysis products (*19*, *29*) and the conformation of myosin with hydrolysis products ADP·P$_i$ bound would be expected

to be essentially the same (*22*). The more surprising observation is that the helical order displayed with ADP·V_i bound is temperature-dependent, and at low temperatures (~5 °C), the myosin heads are disordered. Similarly, with AMP-PNP or ADP·BeF_x bound, we observed a substantial degree of order at temperatures around 35 °C and observed that the amount of order was markedly temperature-dependent. These results argue cogently that the disorder ⇄ order transition is not *directly* associated with nucleoside triphosphate hydrolysis, but rather with a change in the myosin conformation.

Compelling evidence that the M* (closed) conformation is required for order is that for a given temperature the relative abilities of different ligands to promote helical order are strikingly similar to their relative abilities to promote the $M^{\dagger} \rightleftarrows M^*$ (closed) transition. The order for ligands of increasing effectiveness at promoting order we have found in this and previous work (*11*) is as follows: none ~ ADP ~ ATPγS ~ GTP < ATP (unhydrolyzed) ~ AMP-PNP ~ ADP·BeF_x < ADP·V_i < ADP·P_i < CDP·P_i. This is entirely consistent with the relative order of ligands at promoting the formation of the closed conformation. For example, in the absence of ligands, the M (apo) conformation of myosin predominates (*1*, *2*), while with ADP and ATPγS, the $M^{\dagger}$ conformation of the myosin predominates even at higher temperatures (*1*−*3*, *22*). Under all these conditions, we have observed only helical disorder. Studies of the $M^{\dagger} \rightleftarrows M^*$ transition in the presence of GTP have not yet been carried out. However, the equilibrium for the hydrolysis step lies strongly in favor of M·GTP rather than M·GDP·P_i (*42*, *43*) so that by implication the $M^{\dagger} \rightleftarrows M^*$ transition is unfavorable in the presence of this nucleotide; correspondingly, we have observed only helical disorder in the presence of GTP (*11*). In Reanalyzing Data on the Variation with Temperature of K_{ord}^{app} and K_{hyd}^{app}, we calculate $K_{\dagger *}^{app}$ for myosin with bound unhydrolyzed ATP to be 0.20 for rabbit S1 at 25 °C, similar to the value (0.4) previously deduced (*1*) for *Dicytostelium* S1. With AMP-PNP and ADP·BeF_x, the $M^{\dagger} \rightleftarrows M^*$ transition is similarly poised. Málnási-Csizmadia et al. (*1*) found that at each temperature the equilibrium constant for ADP·BeF_x was comparable to that of AMP-PNP; at 5 °C $K_{\dagger *}^{app}$ was 0.20 and 0.11 and at 25 °C 1.74 and 1.06, respectively. This is in good agreement with the present results. Our results are also consistent with the observations by Schrumf and Wray (*12*) that higher temperatures were needed to observe order with ADP·BeF_x than with ATP. The equilibrium constant of the $M^{\dagger} \rightleftarrows M^*$ transition with bound ADP·V_i has yet to be determined, but there are indications from fluorimetric measurements (*1*) that for this complex the M* (closed) conformation is favored more than with ADP·BeF_x, consistent with our observations. In the presence of ATP (with bound ATP in equilibrium with bound products), the M* (closed) conformation is strongly favored at higher temperatures with a $K_{\dagger *}^{app}$ of 45 for *Dictyostelium* S1 at 25 °C (*1*, *2*) or ~97 for rabbit myosin (see above); under these conditions, we found a high level of helical order. Finally, although no value of $K_{\dagger *}^{app}$ has been determined for CTP, the equilibrium of the hydrolysis step is known to be even higher than for ATP (*43*), and hence taken with the results of Málnási-Csizmadia et al. (*1*, *2*), $K_{\dagger *}^{app}$ should be higher than for ATP. Correspondingly, especially at a low temperature (5 °C), we observed that CTP gives substantially more order than ATP (*11*).

It is interesting to note that the effectiveness of different ligands at promoting helical order is almost identical to their effectiveness in decreasing the average distance between the active site and the regulatory light chain observed by Xiao et al. (*44*). The varying average distances could arise from a changing proportion of two conformations, with the open conformation having a distance that is longer than that of the closed conformation. According to this interpretation, the close correlation between helical order and the measured distances is consistent with the idea that filament order requires a closed myosin conformation.

Not only can the relative effectiveness of the ligands at promoting order be explained in terms of their effectiveness at promoting the $M^{\dagger} \rightleftarrows M^*$ transition, but there is a growing understanding of the underlying structural basis for this ordering. It is thought that a hydrogen bond between Gly457 of switch II and the γ-phosphate group of ATP (or P_i in the products) contributes to the stabilization of the closed conformation (*18*). That hydrogen bond could not be formed with ADP alone, explaining why ADP stabilizes the $M^{\dagger}$ conformation instead. The hydrogen bond would be weak if the acceptor were an S atom as in ATPγS and stronger if the acceptor were an F or O atom as in ADP·BeF_x, AMP-PNP, or ATP.

Comparison of Hypotheses. Our experiments with nonhydrolyzable analogues favor the hypothesis that helical order requires the closed conformation rather than the hypothesis that helical order requires the products of ATP hydrolysis in the active site. But for resting muscle, are the predictions made by the two hypotheses very different? When it was supposed that conformational change was tightly coupled to hydrolysis ($M^{\dagger}$·ATP = M*·ADP·P_i), the two hypotheses were necessarily equivalent; temperature affected both the conformational transition and the hydrolysis of ATP equally. However, once it is accepted that the coupling between conformation and ATP hydrolysis is not so tight, the hypotheses are no longer equivalent since the species in the closed conformation are M*·ADP·P_i and M*·ATP, while the species containing bound ADP·P_i are M*·ADP·P_i and $M^{\dagger}$·ADP·P_i and K_{hyd}^{app} is not equal to $K_{\dagger *}^{app}$ (see the Appendix). It is true that as the coupling constant is high, $M^{\dagger}$·ATP is the major species at low temperatures and M*·ADP·P_i at high temperatures, so the quantitative predictions the two hypotheses make do not greatly differ except at extremes of temperature (Figure 5). Nevertheless, mechanistically the hypotheses differ substantially. The hypothesis that order depends on the products of ATP hydrolysis being in the active site requires that temperature primarily affects the equilibrium of the hydrolysis step rather than the conformational transition, contrary to experiment (*1*, *2*). The question of how the contents of the active site could possibly affect helical order, other than by influencing myosin conformation, would also arise. In contrast, the hypothesis that order depends on the closed conformation is fully consistent with the observation that temperature affects the $M^{\dagger} \rightleftarrows M^*$ conformational transition (*1*−*3*) and provides a structural basis for understanding the temperature dependence of helical order.

A Single Ligand Induces Multiple Conformations of Myosin. One outcome of this study was our deduction that

with each of the analogues bound at the active site, three states (A−C) coexist, both in *Dictyostelium* myosin in solution and in rabbit myosin filaments. The C state is the only state with high fluorescence and high order and can therefore be assigned to the M* (closed) conformation, but the nature of the A and B states is less clear. Since the solution studies were performed on a *Dictyostelium* mutant with only one tryptophan residue positioned on the relay loop near the converter subdomain, the conformation of the A and B states must differ from the M* (closed) conformation. A and B have a large enthalpy difference of 154 kJ/mol, consistent with them having different conformations, although the structural basis for this is unknown. With bound ATP, or an ATP analogue, the equilibrium of the $M \rightleftarrows M^{\dagger}$ transition lies strongly in favor of $M^{\dagger}$ (*1*, *2*), implying that neither A or B has the M (apo) conformation. This suggests that the $M^{\dagger}$ conformation exists in two states (A and B). This is consistent with the conclusions of (*65*) who followed the binding of ATP or ADP to a *Dictyostelium* mutant myosin head with a single tryptophan (W129) close to the active site. They found that the binding of ATP or ADP was best modeled as a three-step process effectively resolving the former $M^{\dagger}$ conformation into two states (M_1 and M_2) in rapid equilibrium. It is therefore attractive to suggest that our A and B states are the same as their M_1 and M_2 states.

In the introduction, the $M^{\dagger}$ solution conformation was tentatively assigned to the third detached conformation of the myosin head (*25*, *26*). This was based on the following evidence. In solution, with ADP bound, the major conformation present is $M^{\dagger}$, with the M conformation as a minor species (*1*, *2*). In the presence of ADP, the myosin head has been crystallized in the open conformation (for both *Dictyostelium* and scallop) and in the detached conformation (scallop only) (*25*, *26*, *30*). In solution with the ATP analogues AMP-PNP or ADP·BeF_x bound, the myosin head exists principally as an equilibrium mixture of the $M^{\dagger}$ and M* conformations, with M as a minor species (*1*, *2*). Correspondingly with ADP·BeF_x bound, the head has been crystallized in all three conformations (*18*, *21*, *26*). With AMP-PNP bound, the head has been crystallized in the open conformation (*Dictyostelium*) and detached conformation (scallop) (*26*, *30*). All this suggested that the $M^{\dagger}$ solution conformation could be assigned to the detached crystal conformation. This assignment is supported by the fact that in the detached conformation the SH1 helix is melted (*25*) and that in the presence of ADP (where the $M^{\dagger}$ conformation predominates) the SH1 and SH2 sulfhydryl groups of rabbit myosin can more readily be cross-linked (*70*, *71*). Now that the $M^{\dagger}$ conformation has been resolved into two states, it remains to be determined which of them should be assigned to the detached crystal conformation and how these two states differ.

The crystal structures of myosin have largely been interpreted to mean that the conformation of myosin was absolutely determined by the nature of the ligand bound (see, for example, refs *18* and *26*). With no ligands bound or with bound ATP (or ATP analogues), the myosin heads crystallized in the open conformation, and with analogues of the transition state, they crystallized in the closed conformation. However, several recent X-ray crystallographic studies have given results that do not fit this simple picture. The *Dictyostelium* motor domain with ADP·BeF_x bound has been crystallized in the closed (*22*) as well as the open conformation (*18*). Similarly, scallop S1 with ADP bound has been crystallized in both the detached and open conformations (*26*). Third, the chicken smooth motor domain attached to the essential light chain domain crystallized in the closed conformation whether ADP·AlF_4 (a transition state analogue) or ADP·BeF_x (an ATP analogue) was bound (*21*). These results, however, can be explained rather well by the concept that one ligand can induce multiple conformations.

A characteristic of the transitions between these conformations is that the equilibrium constants, with the possible exception of when ATP is the ligand, are relatively low-energy transitions with equilibrium constants in the range of 1−10. A similar set of low-energy transitions was observed by Shih et al. (*45*) by FRET analysis of donor and acceptors attached to genetically engineered cysteine residues of expressed *Dictyostelium* myosin.

Mechanism of Ordering. We need to understand how the conformation of the heads affects the degree of order and the structure of the ordered and disordered states. We have argued that the closed conformation is required for helical order, but it does not necessarily follow that *all* heads in the closed conformation are ordered. A key question is whether helical ordering in the filament involves an additional step beyond the formation of the closed conformation. Two alternative models can be proposed. In the first model, heads in the $M^{\dagger}$ conformation on the surface of the filament are disordered, while those in the M* (closed) conformation are always ordered. In such a model, the equilibrium constant between the $M^{\dagger}$ and M* conformations is not altered by assembling the molecules into the filament (i.e., the $M^{\dagger}$ and M* conformations are stabilized to the same extent) and $K_{\mathrm{ord}}^{\mathrm{app}}$ is identical to the value of $K_{\dagger *}^{\mathrm{app}}$ found for S1.

Alternatively, it is possible that, in the filament, heads in the M* (closed) conformation occur as an equilibrium mixture of disordered and ordered states. For this type of model

$$K_{\mathrm{ord}}^{\mathrm{app}} = \frac{K_{\dagger *}^{\mathrm{app}} K_{\mathrm{ord}}^{*}}{1 + K_{\dagger *}^{\mathrm{app}}}$$

where K_{ord}^{*} is the equilibrium constant for the ordering of heads in the M* (closed) conformation. The ordering step might, for example, involve the heads in the M* (closed) conformation binding to the heads, head−tail junctions, or tails of neighboring molecules in the filament, thereby stabilizing the position of the heads. In the $M^{\dagger}$ conformation, in contrast, if no such interaction could occur, the heads would be more mobile and might even move out to higher radii by the hinging out of the subfragment-2 regions of their tails. However, we note that in Figure 5 our experimentally determined values of $K_{\mathrm{ord}}^{\mathrm{app}}$ for ATP fall very close to the theoretical line derived from the loose-coupling model for the variation with temperature of $K_{\dagger *}^{\mathrm{app}}$ for single heads, so $K_{\mathrm{ord}}^{\mathrm{app}} = K_{\dagger *}^{\mathrm{app}}$, implying that all, or nearly all, the heads in the M* (closed) conformation are ordered.

We also note that the enthalpy changes for the transitions between myosin conformations (ΔH_{AB}, ΔH_{BC}, and ΔH_{AC}) are independent of the bound ligand, and they are the same for the disorder $\rightleftarrows$ order transition and for the conformational changes in solution. This implies that the same underlying

processes are involved. Since no filament structure is present in the solution studies, it is unlikely that the disorder ⇄ order transition in the thick filament involves processes other than conformational changes in myosin. Therefore, we conclude that no additional ordering step is required.

Structural Origin of the Disorder ⇄ Order Transition. To explain why in the filament the M* (closed) conformation, but not the $M^{\dagger}$ conformation, is *always* an ordered state, we need to discuss the origins of the disorder. In the myosin molecule in solution in the absence of ligands, the two heads appear to be flexibly joined to the tail (*46*−*48*). If the two regulatory light chain domains of the two heads form an interface at the head−tail junction, it is difficult to see how flexing could occur at the head−tail junction itself (*49*). Instead, flexing of the tail might occur just distal to the head−tail junction, and it is even possible that this region of the coiled-coil tail melts (*50*). Within the head, flexing might occur in the regulatory light chain domain where the long α-helix of the lever arm joins the short C-terminal α-helix (*49*), between the regulatory and essential light chains, or between the motor domain and the essential light chain domain (*26*, *49*, *51*, *52*). It has also been shown that the mobility of the catalytic domain is independent of that of the light chain domain (*53*). In the myosin filament, motion of the heads is more restricted than in the free molecules, although motions on the 10 μs time scale still occur (*46*, *54*−*57*). This reduction in flexibility in the filaments might arise because heads in the closed conformation interact with the heads, head−tail junctions, or tails of neighboring molecules. However, if that were the case, the closed conformation would be more favored in the filament than in the molecules. This is incompatible with our data showing the similarity of the enthalpy changes (Figure 3) and $K_{ord}^{app} = K_{\dagger *}^{app}$ (Figure 5) for a single head (see the previous section). Instead, a reduction in the extent of head movement might occur simply because of the stabilization of the tail produced by packing it into the filament backbone. The residual motion observed in the filaments would then be due to flexibility within the heads.

The greater ordering when the heads are in the M* (closed) conformation may be because the heads are inherently stiffer in that conformation, reducing the thermal fluctuations of the heads and thereby the helical arrangement of the myosin molecules in the thick filament becomes clearly observable. An example is when $M^{\dagger}$·ATP attaches to actin, there is a reduction in the extent of thermal motion that leads to an enhancement of the myosin layer lines, compared to the unattached $M^{\dagger}$·ATP state (*38*, *58*). The idea of stiffness change is consistent with the crystal structures of S1, where the four subdomains appear to be only loosely linked in the detached conformation, and possibly also in the open conformation, but closely interact in the closed conformation (*25*). It is important in this context to note that even in the ordered state the heads are by no means completely rigid but show a degree of thermal disorder (*6*, *9*); in the model of Malinchik et al. (*9*) for the ordered state, the root-mean-square isotropic displacement was ∼20 Å.

Physiological Relevance of Helical Ordering. The physiological role of the ordered state is unclear but, because the heads lie close to the filament backbone (*9*), it is likely to reduce the rate of binding of M·ADP·P_i to actin subunits and work in parallel with the tropomyosin−troponin system to maintain the muscle in the relaxed state (*59*, *60*). It is somewhat paradoxical that in contracting muscle, where the attachment of the M*·ADP·P_i intermediate to the thin filaments is a critical step in the cross-bridge cycle, sequestering of the head away from the thin filament would be expected to reduce the rate of this reaction. Escape from the ordered state of such an intermediate by rapid conversion to the $M^{\dagger}$·ADP·P_i conformation may not help since the head may not then be in the right conformation for the start of the power stroke.

The disorder ⇄ order transition could explain the phenomenon that the maximum shortening velocity (V_{max}) in activated, chemically skinned vertebrate skeletal muscle fibers is inhibited by the presence of orthovanadate (*61*). The level of inhibition diminished with increasing temperature, and at ≥25 °C, an increasing level of vanadate no longer inhibits V_{max}. Our results on myosin with bound vanadate suggest that at low temperatures, the disordered myosin heads, extending outward from the filament backbone (*9*), impede filament sliding, whereas at high temperatures, the ordered myosin heads, distributed close to the backbone (*9*), exert little resistance to the movement.

Disordering of the heads may be related to the activation and regulatory mechanisms in a variety of muscles. In synthetic myosin filaments, phosphorylation of the regulatory light chain of the myosin head increases mobility (*62*). In skeletal muscle, phosphorylation of the regulatory light chains of the myosin head causes a shift of the force−pCa relationship to lower Ca^{2+} concentrations and an increased rate of force development (*63*). In this case, the increased disorder of the myosin heads occurs in parallel to this increased sensitivity of tension development to calcium, possibly by increasing the accessibility of the myosin heads to the thin filament (*60*, *64*). In invertebrate muscles, promotion of disorder of the myosin heads appears to have a primary role in regulation. Binding of Ca^{2+} to myosin produces thick filament disorder in scallop muscles where regulation is myosin-linked (*59*, *66*). *Limulus* muscle is activated by, and tarantula muscle modulated by, phosphorylation of the regulatory light chains (*67*), and this has been shown to induce disorder in isolated myosin filaments (*68*, *69*). What has yet to be established is whether the disorder produced under these conditions is of the same nature as that produced in skeletal muscle at low temperatures, and if so whether phosphorylation (or Ca^{2+} binding to scallop myosin) produces disorder by promoting the open conformation.

In summary, by studying the helical order of myosin heads in the thick filament, we have demonstrated that the global conformation of unmodified myosin in a physiological system is sensitive to temperature and the nature of the ligand bound to the active site. Our results strongly support the view that myosin exists in several conformations, the proportions of which depend on temperature as well as the ligand bound. Helical order in the thick filament is a signature for only one of these, the closed conformation. Together with the fluorescence results (*1*−*3*, *23*), our findings provide a consistent explanation of why certain complexes of myosin with nucleotide crystallize in more than one conformation.

ACKNOWLEDGMENT

We thank Drs. John Wray, Clive Bagshaw, Andras Málnási-Csizmadia, and Ralph Yount for helpful discussions. We also thank the scientific staff of beamline X27C at the National Synchrotron Light Source for their expert assistance.

APPENDIX

Modeling of the Effect of Temperature on the M·ATP ⇄ M·ADP·P$_i$ Conformational Equilibria. Here we analyze for the myosin ATPase system how temperature influences the equilibrium constants for the M† ⇄ M* transition and for the hydrolysis of bound ATP. In the model of Málnási-Csizmadia et al. (*1*, *2*), the following equilibria exist, ignoring species produced upon product dissociation such as M·ADP:

$$\begin{array}{ccc} & K^{\dagger}_{hyd} & \\ \mathrm{M^{\dagger}.ATP} & \rightleftarrows & \mathrm{M^{\dagger}.ADP.Pi} \\ \| K_{\dagger *} & & \| cK_{\dagger *} \\ & K^{*}_{hyd} & \\ \mathrm{M^{*}.ATP} & \rightleftarrows & \mathrm{M^{*}.ADP.Pi} \end{array}$$

where $K_{\dagger *}$ is the intrinsic equilibrium constant for the M† ⇄ M* transition with bound ATP, $K^{\dagger}_{hyd}$ that for the hydrolysis step on the M† conformation, and K^{*}_{hyd} that on the M* conformation. We take the M† ⇄ M* transition with bound ADP·P$_i$ to be stabilized by a factor c, the coupling constant, compared with ATP ($c > 1$). Consideration of the equilibrium box shows that $K^{\dagger}_{hyd}$ is related to K^{*}_{hyd} by $cK^{\dagger}_{hyd} = K^{*}_{hyd}$.

Note that inclusion of the hydrolytic step in the M† conformation is made only for generality and should not be taken to imply that this step occurs at an appreciable rate. For simplicity, we assume that temperature primarily affects $K_{\dagger *}$, rather than K^{*}_{hyd} or c. Expressing the equilibrium constant for the M† ⇄ M* transition with bound ATP as a function of absolute temperature T and assuming the enthalpy change for this transition is invariant with temperature, we find

$$K_{\dagger *} = K^{298}_{\dagger *} \exp(-\Delta H/RT + \Delta H/298R)$$

where $K^{298}_{\dagger *}$ is the equilibrium constant for the M† ⇄ M* transition with bound ATP at 298 K.

The equilibrium constant for the M† ⇄ M* transition in the presence of ATP (i.e., when bound ATP and ADP·P$_i$ are in equilibrium) is given by

$$K^{app}_{\dagger *} = \frac{[\mathrm{M^{*}\cdot ATP}] + [\mathrm{M^{*}\cdot ADP\cdot P_i}]}{[\mathrm{M^{\dagger}\cdot ATP}] + [\mathrm{M^{\dagger}\cdot ADP\cdot P_i}]} = \frac{1 + K^{*}_{hyd}}{c + K^{*}_{hyd}} cK_{\dagger *} = \frac{1 + K^{*}_{hyd}}{c + K^{*}_{hyd}} cK^{298}_{\dagger *} \exp(-\Delta H/RT + \Delta H/298R)$$

So the equilibrium constant for the conformational change in the presence of ATP would show the same temperature dependence (as measured by the enthalpy change) as the conformational change with bound ATP.

The apparent equilibrium constant for ATP hydrolysis is given by

$$K^{app}_{hyd} = \frac{[\mathrm{M^{\dagger}\cdot ADP\cdot P_i}] + [\mathrm{M^{*}\cdot ADP\cdot P_i}]}{[\mathrm{M^{\dagger}\cdot ATP}] + [\mathrm{M^{*}\cdot ATP}]} = \frac{K^{*}_{hyd}(1 + cK_{\dagger *})}{c(1 + K_{\dagger *})} = \frac{K^{*}_{hyd}[1 + cK^{298}_{\dagger *} \exp(-\Delta H/RT + \Delta H/298R)]}{c[1 + K^{298}_{\dagger *} \exp(-\Delta H/RT + \Delta H/298R)]}$$

To fit data on the temperature dependence of K^{app}_{hyd}, we therefore need four parameters (ΔH, K^{*}_{hyd}, $K^{298}_{\dagger *}$, and c), but the same four parameters define $K^{app}_{\dagger *}$.

In this scheme, unlike $K^{app}_{\dagger *}$, K^{app}_{hyd} does not have a simple dependence on temperature, and a plot of ln K^{app}_{hyd} versus $1/T$ will be S-shaped. Qualitatively, at low temperatures, the exponential terms in the above equation will be negligible, the myosin will essentially all be in the M† conformation, and the observed hydrolysis equilibrium constant will be the low value ($K^{\dagger}_{hyd}$) for the M† conformation. At high temperatures, the exponential terms will be large, myosin will be nearly all in the M* (closed) conformation, and K^{app}_{hyd} will increase to K^{*}_{hyd}. At intermediate temperatures, the myosin will be in both conformations. Increasing the temperature will increase the proportion of the closed conformation, thereby favoring hydrolysis. So in the intermediate temperature range, K^{app}_{hyd} will increase steeply with temperature. The midpoint of the S shape occurs when $K^{app}_{hyd} = K^{*}_{hyd}/\sqrt{c}$, where the slope is approximately $-\Delta H/[R(1 + 1/\sqrt{c})]$, i.e., a magnitude that is slightly less than the slope ($-\Delta H/R$) of the ln $K^{app}_{\dagger *}$ versus $1/T$ line.

NOTE ADDED AFTER PRINT PUBLICATION

Because of a production error, the artwork portions of Figures 1 and 4 were swapped and the ∂ in the second equation was retained in error in the version published on the Web 12/19/02 (ASAP) and in the January 21, 2003, issue (Vol. 42, No. 2, pp 390−401). The correct electronic version of the paper was published 02/05/03.

REFERENCES

1. Málnási-Csizmadia, A., Pearson, D. S., Kovács, M., Woolley, R. J., Geeves, M. A., and Bagshaw, C. R. (2001) *Biochemistry 40*, 12727−12737.
2. Málnási-Csizmadia, A., Woolley, R. J., and Bagshaw, C. R. (2000) *Biochemistry 39*, 16135−16146.
3. Urbanke, C., and Wray, J. (2001) *Biochem. J. 358*, 165−173.
4. Wray, J. (1987) *J. Muscle Res. Cell Motil. 8*, 62a.
5. Wakabayashi, T., Akiba, T., Hirose, K., Tomioka, A., Tokunaga, M., Suzuki, C., Toyoshima, C., Sutoh, K., Yamamoto, K., Matsumoto, T., Sacki, K., and Amemiya, Y. (1988) in *Molecular Mechanism of Muscle Contraction* (Sugi, H., and Pollack, G. H., Eds.) pp 39−48, Plenum, New York.
6. Lowy, J., Popp, D., and Stewart, A. A. (1991) *Biophys. J. 60*, 812−824.
7. Kensler, R. W., Peterson, S., and Norberg, M. (1994) *J. Muscle Res. Cell Motil. 15*, 69−79.
8. Kensler, R. W., and Woodhead, J. L. (1995) *J. Muscle Res. Cell Motil. 16*, 79−90.
9. Malinchik, S., Xu, S., and Yu, L. C. (1997) *Biophys. J. 73*, 2304−2312.
10. Xu, S., Malinchik, S., Gilroy, D., Kraft, T., Brenner, B., and Yu, L. C. (1997) *Biophys. J. 73*, 2655−2666.
11. Xu, S., Gu, J., Rhodes, T., Belknap, B., Rosenbaum, G., Offer, G., White, H., and Yu, L. C. (1999) *Biophys. J. 77*, 2665−2676.

12. Schrumpf, M., and Wray, J. (1992) *J. Muscle Res. Cell Motil. 13*, 254a.
13. Taylor, E. W. (1977) *Biochemistry 16*, 732−739.
14. White, H. D., and Taylor, E. W. (1976) *Biochemistry 15*, 5818−5826.
15. Bagshaw, C. R., Eccleston, J. F., Eckstein, F., Goody, R. S., Gutfreund, H., and Trentham, D. R. (1974) *Biochem. J. 141*, 351−364.
16. Shriver, J. W., and Sykes, B. D. (1981) *Biochemistry 20*, 2004−2012.
17. Wakabayashi, K., Tokunaga, M., Kohno, I., Sugimoto, Y., Hamanaka, T., Takezawa, Y., Wakabayashi, T., and Amemiya, Y. (1992) *Science 258*, 443−447.
18. Fisher, A. J., Smith, C. A., Thoden, J. B., Smith, R., Sutoh, K., Holden, H. M., and Rayment, I. (1995) *Biochemistry 34*, 8960−8972.
19. Smith, C. A., and Rayment, I. (1996) *Biochemistry 35*, 5404−5417.
20. Mendelson, R. A., Schneider, D. K., and Stone, D. B. (1996) *J. Mol. Biol. 256*, 1−7.
21. Dominguez, R., Freyzon, Y., Trybus, K. M., and Cohen, C. (1998) *Cell 94*, 559−571.
22. Geeves, M. A., and Holmes, K. C. (1999) *Annu. Rev. Biochem. 68*, 687−728.
23. Jahn, W., Urbanke, C., and Wray, J. (1999) Fluorescence temperature jump studies of myosin S1 structure, *Biophys. J. 76*, A146.
24. Bauer, C. B., Holden, H. M., Thoden, J. B., Smith, R., and Rayment, I. (2000) *J. Biol. Chem. 275*, 38494−38499.
25. Houdusse, A., Kalabokis, V. N., Himmel, D., Szent-Györgyi, A. G., and Cohen, C. (1999) *Cell 97*, 459−470.
26. Houdusse, A., Szent-Gyorgyi, A. G., and Cohen, C. (2000) *Proc. Natl. Acad. Sci. U.S.A. 97*, 11238−11243.
27. Rayment, I., Rypniewski, W., Schmidt-Base, K., Smith, R., Tomchick, D. R., Benning, M. M., Winkelmann, D. A., Wesenberg, G., and Holden, H. M. (1993) *Science 261*, 50−58.
28. Goodno, C. C., and Taylor, E. W. (1982) *Proc. Natl. Acad. Sci. U.S.A. 79*, 21−25.
29. Deng, H., Wang, J., Callender, R. H., Grammer, J. C., and Yount, R. G. (1998) *Biochemistry 37*, 10972−10979.
30. Gulick, A. M., Bauer, C. B., Thoden, J. B., and Rayment, I. (1997) *Biochemistry 36*, 11619−11628.
31. Frisbie, S. M., Xu, S., Chalovich, J. M., and Yu, L. C. (1998) *Biophys. J. 74*, 3072−3082.
32. Resetar, A. M., and Chalovich, J. M. (1995) *Biochemistry 34*, 16039−16045.
33. Frisbie, S. M., Chalovich, J. M., Brenner, B., and Yu, L. C. (1997) *Biophys. J. 72*, 2255−2261.
34. Goodno, C. C. (1982) *Methods Enzymol. 85*, 116−123.
35. Werber, M. M., Peyser, Y. M., and Muhlrad, A. (1992) *Biochemistry 31*, 7190−7197.
36. Brenner, B., Yu, L. C., and Chalovich, J. M. (1991) *Proc. Natl. Acad. Sci. U.S.A. 88*, 5739−5743.
37. Brenner, B., Yu, L. C., Greene, L. E., Eisenberg, E., and Schoenberg, M. (1986) *Biophys. J. 50*, 1101−1108.
38. Xu, S., Gu, J., Melvin, G., and Yu, L. C. (2002) *Biophys. J. 82*, 2111−2122.
39. Yount, R. G., Ojala, D., and Babcock, D. (1971) *Biochemistry 10*, 2490−2496.
40. Muhlrad, A., Cheung, P., Phan, B. C., Miller, C., and Reisler, E. (1994) *J. Biol. Chem. 269*, 11852−11858.
41. Takemori, S., Yamaguchi, M., and Yagi, N. (1995) *J. Biochem. 117*, 603−608.
42. Eccleston, J. F., and Trentham, D. R. (1979) *Biochemistry 18*, 2896−2904.
43. White, H. D., Belknap, B., and Webb, M. R. (1997) *Biochemistry 36*, 11828−11836.
44. Xiao, M., Li, H., Snyder, G. E., Cooke, R., Yount, R. G., and Selvin, P. R. (1998) *Proc. Natl. Acad. Sci. U.S.A. 95*, 15309−15314.
45. Shih, W. M., Gryczynski, Z., Lakowicz, J. R., and Spudich, J. (2000) *Cell 102*, 683−694.
46. Mendelson, R. A., Morales, M. F., and Botts, J. (1973) *Biochemistry 12*, 2250−2255.
47. Elliott, A., and Offer, G. (1978) *J. Mol. Biol. 123*, 505−519.
48. Walker, M., Knight, P., and Trinick, J. (1985) *J. Mol. Biol. 184*, 535−542.
49. Offer, G., and Knight, P. (1996) *J. Mol. Biol. 256*, 407−416.
50. Knight, P. J. (1996) *J. Mol. Biol. 255*, 269−274.
51. Burgess, S. A., Walker, M. L., White, H. D., and Trinick, J. (1997) *J. Cell Biol. 139*, 675−681.
52. Roopnarine, O., Szent-Györgyi, A. G., and Thomas, D. D. (1998) *Biochemistry 37*, 14428−14436.
53. Adhikari, B., Hideg, K., and Fajer, P. G. (1997) *Proc. Natl. Acad. Sci. U.S.A. 94*, 9643−9647.
54. Mendelson, R., and Cheung, P. H. (1978) *Biochemistry 17*, 2139−2148.
55. Eads, T. M., Thomas, D. D., and Austin, R. H. (1984) *J. Mol. Biol. 179*, 55−81.
56. Cooke, R., and Thomas, D. (1980) *Fed. Proc. 39*, 1962.
57. Barnett, V. A., and Thomas, D. D. (1987) *Biochemistry 26*, 314−323.
58. Gu, J., Xu, S., and Yu, L. C. (2002) *Biophys. J. 82*, 2123−2133.
59. Frado, L.-L. Y., and Craig, R. (1989) *J. Cell Biol. 109*, 529−538.
60. Levine, R. J., Yang, Z., Epstein, N. D., Fananapazir, L., Stull, J. T., and Sweeney, H. L. (1998) *J. Struct. Biol. 122*, 149−161.
61. Pate, E., Wilson, G. J., Bhimani, M., and Cooke, R. (1994) *Biophys. J. 66*, 1554−1562.
62. Adhikari, B. B., Somerset, J., Stull, J. T., and Fajer, P. G. (1999) *Biochemistry 38*, 3127−3132.
63. Sweeney, H. L., and Stull, J. T. (1990) *Proc. Natl. Acad. Sci. U.S.A. 87*, 414−418.
64. Levine, R. J., Kensler, R. W., Yang, Z., Stull, J. T., and Sweeney, H. L. (1996) *Biophys. J. 71*, 898−907.
65. Kovács, M., Málnási-Csizmadia, A., Woolley, R. J., and Bagshaw, C. R. (2002) *J. Biol. Chem. 277*, 28459−28467.
66. Vibert, P., and Craig, R. (1985) *J. Cell Biol. 101*, 830−837.
67. Sellers, J. R., Pato, M. D., and Adelstein, R. S. (1981) *J. Biol. Chem. 256*, 13137−13142.
68. Craig, R., Padron, R., and Kendrick-Jones, J. (1987) *J. Cell Biol. 105*, 1319−1327.
69. Levine, R. J., Chantler, P. D., Kensler, R. W., and Woodhead, J. L. (1991) *J. Cell Biol. 113*, 563−572.
70. Wells, J. A. (1980) *Biochemistry 19*, 1711−1717.
71. Riesler, E., Burke, M., and Harrington, W. F. (1977) *Biochemistry 16*, 5187−5191.

BI026085T